9-1-2005

The Octarepeat Domain of the Prion Protein Binds Cu(II) with Three Distinct Coordination Modes at pH 7.4

Madhuri Chattopadhyay
University of California - Santa Cruz

Eric D. Walter
University of California - Santa Cruz

Dustin J. Newell
University of California - Santa Cruz

Pilgrim J. Jackson
University of California - Santa Cruz

Eliah Aronoff-Spencer
Albert Einstein College of Medicine

See next page for additional authors

Accepted version. *Journal of the American Chemical Society,* Vol. 127, No. 36 (September 2005): 12647-12656. DOI.
Brian Bennett was affiliated with Medical College of Wisconsin at the time of publication.

The Octarepeat Domain of the Prion Protein Binds Cu(II) with Three Distinct Coordination Modes at pH 7.4

Madhuri Chattopadhyay
Department of Chemistry & Biochemistry,
University of California,
Santa Cruz, CA
Eric D. Walter
Department of Chemistry & Biochemistry,
University of California,
Santa Cruz, CA
Dustin J. Newell
Department of Chemistry & Biochemistry,
University of California,
Santa Cruz, CA
Pilgrim J. Jackson
Department of Chemistry & Biochemistry,
University of California,
Santa Cruz, CA

Journal of the American Chemical Society, Vol 127, No. 36 (September 14, 2005): pg. 12647-12656. DOI.

Eliah Aronoff-Spencer
Department of Physiology and Biophysics,
Albert Einstein College of Medicine,
Bronx, NY
Jack Peisach
Department of Physiology and Biophysics,
Albert Einstein College of Medicine,
Bronx, NY
Gary J. Gerfen
Department of Physiology and Biophysics,
Albert Einstein College of Medicine,
Bronx, NY
Brian Bennett
Department of Biophysics, Medical College of Wisconsin,
Milwaukee, WI
William E. Antholine
Department of Biophysics, Medical College of Wisconsin,
Milwaukee, WI
Glenn L. Millhauser
Department of Chemistry & Biochemistry,
University of California,
Santa Cruz, CA

Abstract

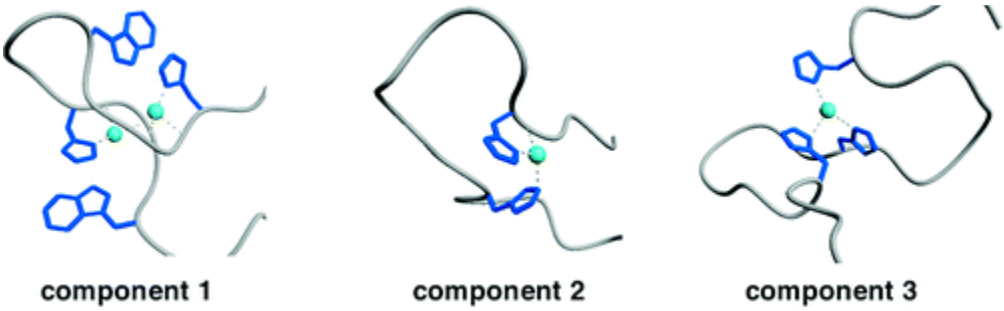

Journal of the American Chemical Society, Vol 127, No. 36 (September 14, 2005): pg. 12647-12656. DOI.

The prion protein (PrP) binds Cu^{2+} in its N-terminal octarepeat domain. This unusual domain is comprised of four or more tandem repeats of the fundamental sequence PHGGGWGQ. Previous work from our laboratories demonstrates that at full copper occupancy, each HGGGW segment binds a single Cu^{2+}. However, several recent studies suggest that low copper occupancy favors different coordination modes, possibly involving imidazoles from histidines in adjacent octapeptide segments. This is investigated here using a combination of X-band EPR, S-band EPR, and ESEEM, along with a library of modified peptides designed to favor different coordination interactions. At pH 7.4, three distinct coordination modes are identified. Each mode is fully characterized to reveal a series of copper-dependent octarepeat domain structures. Multiple His coordination is clearly identified at low copper stoichiometry. In addition, EPR detected copper−copper interactions at full occupancy suggest that the octarepeat domain partially collapses, perhaps stabilizing this specific binding mode and facilitating cooperative copper uptake. This work provides the first complete characterization of all dominant copper coordination modes at pH 7.4.

Introduction

Conversion of the prion protein (PrP) from its normal cellular form (PrP^C) to the scrapie form (PrP^{Sc}) is responsible for a class of infectious, neurodegenerative diseases referred to as the transmissible spongiform encephalopathies (TSEs).[1,2] The TSEs include mad cow disease (BSE), scrapie in goats and sheep, chronic wasting disease (CWD) in deer and elk, and, in humans, kuru and Creutzfeldt−Jakob disease (CJD). In contrast to other known infectious diseases resulting from viruses or bacteria, the transmissible agent requires only protein in the form of β-sheet rich PrP^{Sc}.[3]

PrP^C is found in a wide range of tissues. Within the central nervous system, it is localized primarily at presynaptic membranes,[4,5] attached through a glycophosphatidylinositol (GPI) anchor.[6] The normal function of PrP^C in healthy tissues is not known. However, since the landmark work of Brown et al. in 1997,[7] accumulating evidence links PrP^C function to its ability to bind Cu^{2+}. To refine possible physiological roles for PrP^C, there are intensive efforts to clearly define the Cu^{2+} coordination environment.[8-25] Mature PrP^C is a 209 amino acid (after removal of the signal peptide) glycoprotein with a folded C-terminus and an unstructured (in the absence of Cu^{2+}) N-terminus.[26] A variety of experiments using peptides and recombinant PrP (rPrP) find that most copper ions bind in the N-terminal octarepeat domain composed of four or five tandem repeats of the fundamental eight-

Journal of the American Chemical Society, Vol 127, No. 36 (September 14, 2005): pg. 12647-12656. DOI.

residue sequence PHGGGWGQ (residues 60−91 in the four octarepeat hamster sequence).[13,14,17,20] Recent experiments point to an additional binding site involving either His96[11,20] or His111,[16] although there is current disagreement as to its exact location.[16] In the fully occupied octarepeat domain, each octarepeat segment binds a single Cu^{2+} ion. As demonstrated by our laboratories using EPR and X-ray crystallography, copper forms a pentacoordinate complex involving the specific residues HGGGW.[8,10] Equatorial coordination involves the His imidazole, deprotonated amides from the following two Gly residues and the amide carbonyl from the second glycine. An oxygen from a water molecule coordinates axially and bridges to the NH of the Trp indole.

Although the detailed features of fully copper-occupied PrP^C are now well established, little is known about the copper coordination geometry, or the structure of the N-terminal domain, at intermediate Cu^{2+} occupancy. Moreover, no experiments thus far have elucidated any possible molecular interactions among the distinct copper sites in the fully occupied state. These issues are vital for understanding how PrP^C responds to localized changes in Cu^{2+} concentrations that are known to take place in the central nervous system, particularly at synapses.[5] For example, PrP^C is constitutively cycled through endocytosis. Addition of Cu^{2+} rapidly stimulates this process, resulting in significant PrP^C internalization.[27] Mutant PrP^C lacking the N-terminal octarepeat domain is less efficiently endocytosed in the presence of copper. It has been proposed that elevation of the Cu^{2+} concentration introduces a structural change in PrP^C that increases its association with membrane components targeted for compartmentalization to the endosome.[27]

PrP^C is also implicated in protecting neurons against copper-mediated oxidative stress. Because of its intrinsic redox activity involving the oxidation states Cu^{2+} and Cu^{+}, high concentrations of uncomplexed or weakly complexed copper contribute to the production of reactive oxygen species, which are toxic to cells. A growing number of experiments indeed show that wild-type neurons in culture are more resistant to copper toxicity than are cells lacking PrP.[5,28,29] Correspondingly, comparison of tissues between normal mice and PrP knockouts reveals extensive oxidative damage in the latter.[30]

Journal of the American Chemical Society, Vol 127, No. 36 (September 14, 2005): pg. 12647-12656. DOI.

Together, these findings suggest a copper buffering role for PrP where the protein protects cells from uncomplexed Cu^{2+}. Mechanistic support for this type of function comes from several copper binding experiments that reveal micromolar dissociation constants, well matched to extracellular Cu^{2+} levels,[23,31,32] with significant positive binding cooperativity,[23,32] suggesting that PrP^C is able to alter structure from a state of low copper affinity to a multiply occupied state of high affinity, over a narrow copper concentration range.

At full occupancy, each octarepeat histidine coordinates to single Cu^{2+}, as described above. However, at intermediate occupancy, a single Cu^{2+} may be coordinated by two or more His imidazoles.[15,33,34] Although a detailed mechanism has not yet been proposed, significant changes in octarepeat organization may ultimately explain the molecular basis for the proposed binding cooperativity.[33] Alternatively, distinct binding modes as a function of copper occupancy may point to a copper sensing role for PrP^C, or even a protein that carries out several different functions depending on the extracellular Cu^{2+} concentration.

Studies from our laboratories, using multi-frequency and pulsed EPR, along with designed libraries of isotopically labeled peptides, have defined the coordination mode in the fully occupied octarepeat domain as described above.[8,10,17] Additional studies with folded, recombinant PrP^C demonstrate that this defined coordination mode is preserved in the full-length protein.[11] In the course of our studies with copper complexes of the octarepeat domain, corresponding to PrP(57−91),[8] and with rPrP,[11] we identified EPR spectra reflecting a superposition consistent with two or more bound species. Only the dominant binding mode at full occupancy has thus far been characterized. In light of the numerous structural and physiological issues above, we investigate here the structural features over a range of Cu^{2+} concentrations. EPR spectra clearly identify three distinct binding modes at pH 7.4. Using a combination of EPR techniques, along with a variety of octarepeat domain constructs and isotopic labeling, we characterize the coordination features of each mode. Moreover, we reinvestigated spectra obtained at high copper occupancy and find evidence for close copper−copper contacts consistent with a packing interaction in the copper loaded N-terminal octarepeat domain.

Journal of the American Chemical Society, Vol 127, No. 36 (September 14, 2005): pg. 12647-12656. DOI.

Materials and Methods

Peptide Synthesis and Purification. All peptides containing common amino acids were prepared using fluorenylmethoxycarbonyl (Fmoc) methods, as described previously.[8,10] Peptides were acetylated at the N-terminus and amidated at the C-terminus. *N*-Methylated glycine was introduced by the coupling of bromoacetic acid to the preceding glycine using 1,3-diisopropylcarbodiimide (DIC)/*N*,*N*-diisopropylethylamine (DIEA) in dichloromethane for 30 min, followed by reaction with methylamine in tetrahydrofuran (THF) for another 30 min.[35] The next amino acid was coupled in the conventional fashion. To methylate the amide nitrogen of histidine, the Fmoc group was removed and the resulting free N-terminal amine was protected using *o*-nitrobenzenesulfonyl chloride (3 equiv) and collidine (3 equiv) for 30 min.[36] The methyl group was then added by coupling with 3 equiv of methyl-4-nitrobenzenesulfonate in the presence of 3 equiv of 1,3,4,6,7,8-hexahydro-1-methyl-2*H*-pyrimido[1,2-*a*]-pyrimidine (MTBD) for30 min. The N-terminal nitrogen was then deprotected using 1,8-diazabicyclo[5.4.0]-undec-7-ene (DBU) (3 equiv) and β-mercaptoethanol (3 equiv) for 30 min. All peptides were acetylated prior to cleavage and purified by reverse-phase HPLC.

Electron Paramagnetic Resonance (EPR) Spectroscopy. All samples were prepared with degassed buffer containing 25 mM *N*-ethylmorpholine (NEM) buffer and 20% glycerol (v/v) where the glycerol served as a cryoprotectant.[8] X-band spectra (frequency = 9.43 GHz, microwave power in the range 0.6−5.0 mW, modulation amplitude in the range 5.0−15 G) were acquired using a Bruker EleXsys 500 spectrometer and a TE_{102} or SHQ (Bruker) cavity equipped with a variable temperature controller. ^{63}Cu (99.62%, Cambridge Isotope Laboratories) was used to avoid inhomogeneous broadening of the S-band EPR lines that would otherwise be present with the mixture of naturally occurring isotopes. S-band spectra (3.5 GHz) were acquired in D_2O solution at 133 K using a loop gap resonator as part of a specially designed spectrometer housed at the Biomedical ESR Center at the Medical College of Wisconsin. Three-pulse ESEEM measurements were obtained at 4.2 K on an X-band pulsed-EPR spectrometer located at the Albert Einstein College of Medicine. The instrument, cavity, and resonator were constructed in-house and have

Journal of the American Chemical Society, Vol 127, No. 36 (September 14, 2005): pg. 12647-12656. DOI.

been previously described.[37,38] Data were obtained at $g_\perp$, the point of greatest spectral intensity (3280 G at 9.47 GHz). Data processing to attain frequency domain spectra for three-pulse ESEEM was carried out using software described in previous work.[39] Echo detected spectra were obtained at 6 K with a repetition rate of 33 Hz and 30 averages per magnetic field point. Additional experimental parameters for all pulsed experiments are provided in figure legends.

EPR spectra were simulated using previously reported procedures[40] using the program XSophe (Bruker Biospin)[41] and employing the spin Hamiltonians

$$\mathbf{H} = \beta g \cdot H \cdot S + S \cdot A \cdot I$$

and

$$\mathbf{H} = \beta g_1 \cdot H \cdot S_1 + S_1 \cdot A_1 \cdot I_1 + \beta g_2 \cdot H \cdot S_2 + S_2 \cdot A_2 \cdot I_2 + S_1 \cdot J \cdot S_2$$

for one- and two-copper simulations, respectively. J contains both isotropic and anisotropic coupling terms between the two $S = {}^1/_2$ spins. Signals were simulated assuming equivalent g and A for the two individual Cu^{2+} ions. The appearance of the $g \approx 2$ region of the spectra due to spin-coupled Cu^{2+} ions was largely dictated by $g_\perp$, and while the simulations were sensitive to the inter-Cu(II) distance, they did not provide good estimates for $g_\parallel$ and $A_\parallel$ in this case. In contrast, the half field simulations provided good estimates for $g_\parallel$ and $A_\parallel$, in addition to the inter-Cu^{2+} distance. An isotropic exchange coupling was assumed with $JS_1S_2 > \beta gHS$ (an arbitrary value of 35 cm^{-1} was used).

Structure Calculations. Calculations for the various binding modes used the CYANA torsional dyanamics program.[42] A histidine residue with copper bound was added to the CYANA library. The copper ion was placed 2.0 Å from the Histidine Nδ atom consistent with the HGGGW crystal structure. Each calculation maintained fixed peptide bond distances and angles and used upper limit restraints and torsion angle dynamics to produce a low energy structure. In each case, 50 structures were calculated, and the lowest energy conformer is shown (Figure 8). The following upper and lower limit restraint files were used for the various components. Component 1 maintained the

Journal of the American Chemical Society, Vol 127, No. 36 (September 14, 2005): pg. 12647-12656. DOI.

structure of the HGGGW as it appears in the crystal structure, and additionally included a fixed copper−copper distance of 4.0 Å between two of the centers. Component 2 used a fixed 2.0 Å distance between each copper atom and the histidine amide nitrogen and Nδ, and a 2.4 Å distance to the Nε of the preceding histidine. Component 3 has a single copper coordinated to three histidines with a fixed distance of 2.0 Å between the Cu^{2+} and the histidine Nε atoms.

Results

Cu^{2+} binds primarily within the octarepeat domain, residues 60−91 in hamster PrP (SHaPrP), consisting of four tandem repeats of the fundamental eight-residue sequence PHGGGWGQ (Table 1).[11,17] There is an additional binding site at His96,[11,16] and perhaps at His111,[16] although there is currently disagreement about the precise location of this nonoctarepeat copper. It has been noted previously that EPR spectra reflect a change in coordination geometry as a function of relative Cu^{2+}/PrP concentrations, suggesting alternate binding modes at low copper levels.[8] This is investigated here with a series of EPR spectra obtained as a function of copper concentration at pH 7.4. The soluble octarepeat domain construct, PrP(23−28, 57−91), was used to yield high signal/noise spectra without interference from the nonoctarepeat binding sites.[8] Spectra obtained from 0.25 to 2.0 equiv of Cu^{2+} (added to a solution containing 200 μM peptide), in increments of 0.25 equiv, are shown in Figure 1. At 2.0 equiv and above, the spectra are dominated by a signal previously referred to as component 1.[8,11] (A more extensive set of spectra up to 6.0 equiv of Cu^{2+} is in the Supporting Information.) However, at low occupancy, two additional EPR spectra emerge, and this is clearly seen in the expansion of the low field spectral range showing the $m_I = -3/2$ and $m_I = -1/2$ hyperfine lines. The additional spectrum observed between approximately 1.0 and 2.0 equiv is referred to as component 2.[8] At 1.0 equiv and below, a single spectrum, referred to as component 3, dominates. This process is reversible and reveals a coexistence among three distinct copper bound species. Magnetic parameters, $g_\parallel$ and $A_\parallel$, determined from the parallel region of the three spectral components are summarized in Table 2. Below we characterize each of the distinct binding modes.

Journal of the American Chemical Society, Vol 127, No. 36 (September 14, 2005): pg. 12647-12656. DOI.

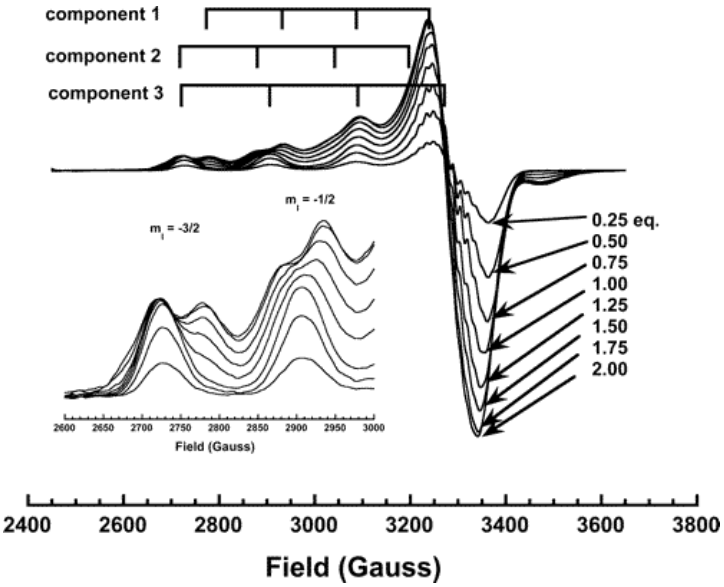

Figure 1 X-band EPR spectra of PrP(23−28, 57−91) (200 μM) as a function of Cu^{2+} concentration, represented in equivalents. Three distinct species are observed, as can be clearly seen in the inset showing an expansion of the $m_I = -3/2$ and $m_I = -1/2$ hyperfine lines. The grids at the top identify the four hyperfine lines arising from coupling to the ^{63}Cu ($I = 3/2$) nucleus for each spectral species. Spectra were obtained at approximately 77 K and v_o = 9.44 GHz.

Table 1. Peptide Sequences[a]

	component		
	1	2	3
KKRPKPWGQ(PHGGGWGQ)$_4$ PrP(23−28, 57−91)	X	X	X
(PHGGGWGQ)$_3$	X	X	X
HGGGWGQPHGGGW	X	X	
PHGGGWGQ	X		
HGGGW	X		
KKRPKPWGQ(PHGXGWGQ)$_4$		X	X
HGXGWGQPHGXGW		X	
HGXGW		X	
HXGGW		X	
HGGGWGQPYGGGW	X		
YGGGWGQPHGGGW	X		
HGGGWGQPYGGGWGQPHGGGW	X		

[a] X = sarcosine (*N*-methylglycine).

Journal of the American Chemical Society, Vol 127, No. 36 (September 14, 2005): pg. 12647-12656. DOI.

Table 2.

	$g_{\parallel}$	A∥ MHz	Gauss	coordination[a]	center charge
component 1	2.24	492	157	3N 1O	0
component 2	2.27	530	167	2N 2O	0[a]
component 3	2.25	576	183	3N 1O or 4N	0 or +1[a]

[a] Assigned using Peisach−Blumberg correlations.[43]

Component 1 Coordination − High Cu^{2+} Occupancy. The local Cu^{2+} coordination environment of component 1 was previously characterized using EPR, including X-band, S-band, and ESEEM, as well as X-ray crystallography.[10] Coordination is localized within the octarepeat subsegment HGGGW and involves the His imidazole and deprotonated amide nitrogens from the following two Gly residues in the equatorial plane, as well as an axial water that hydrogen bonds to the NH of the Trp indole.[10,17]

Table 1 shows a series of PrP-derived peptide constructs along with spectral components observed from titration studies, such as those carried out in Figure 1. (Additional EPR spectra vs added Cu^{2+} are given in the Supporting Information.) As observed in our previous studies, component 1 is found in the minimal binding sequence HGGGW, as well as in all longer constructs including the full, four-octarepeat domain. Moreover, quantitative titration studies showed that each octarepeat binds a single equivalent of Cu^{2+}.[8]

Although the local coordination in component 1 binding is fully elucidated, the relative spatial positioning among the Cu^{2+} containing HGGGW segments is unknown. However, contacts between copper centers, as revealed by dipolar interactions, may be informative, and this is investigated in Figure 2. The EPR spectrum obtained from the octarepeat segment PHGGGWGQ is nearly equivalent to that obtained from the fully occupied octarepeat domain PrP(23−28, 57−91).[8] Both spectra are dominated by component 1 binding, although the octarepeat domain shows residual component 2 binding as well. However, PrP(23−28, 57−91) reveals additional features at approximately 3100 G (where it adds to the $m_I = {}^1/_2$ copper hyperfine line) and 3475 G, as indicated by the arrows. These features are

Journal of the American Chemical Society, Vol 127, No. 36 (September 14, 2005): pg. 12647-12656. DOI.

suggestive of a strongly coupled dipolar spectrum superimposed on the uncoupled component 1 spectrum.[40]

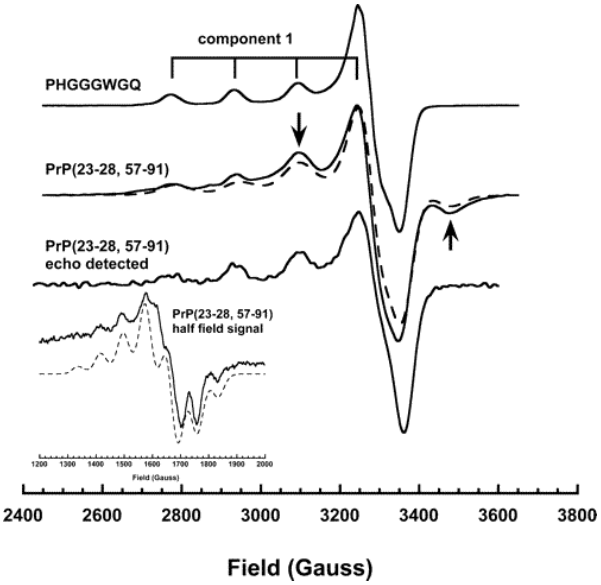

Figure 2 X-band EPR spectra showing the approximate equivalence of fully occupied PrP(23−28, 57−91) and PHGGGWGQ. The spectrum for PrP(23−28, 57−91) also reveals features associated with dipolar coupling (arrows). The echo detected spectrum of PrP(23−28, 57−91), obtained with a two pulse sequence (τ = 140 ns, ν_o = 9.63 GHz, T = 6 K), selects for slowly relaxing species and lacks the dipolar features, thus confirming a spectral superposition. The inset shows the half field signal (ν_o = 9.63 GHz) obtained from PrP(23−28, 57−91) with 2.0 equiv of Cu^{2+}. The simulation (dashed line) for the $g \approx 2$ spectrum was generated with a superposition of a mononuclear species (80%) and a coupled species (20%) using the parameters $g_\parallel$ = 2.227, $g_\perp$ = 2.052, and $A_\parallel$ = 162 G and $g_\parallel$ = 2.176, $g_\perp$ = 2.058, and $A_\parallel$ = 165 G, respectively, and a distance of 6.0 Å. The simulation of the half field signal (dashed line) used $g_\parallel$ = 2.174, $g_\perp$ = 2.058, and $A_\parallel$ = 162 G and a distance of 4.9 Å. In addition, the **g** tensors for the Cu(II) ions were assumed to be collinear with an intercopper vector at a 10° ± 5° angle to the z direction.

To evaluate whether the spectrum of fully occupied PrP(23−28, 57−91) with 2 or more equiv of Cu^{2+} is indeed a superposition of two types of copper centers (noninteracting and dipolar/exchange interacting), an echo detected (ED) spectrum was obtained. Coupling between paramagnetic species via exchange and/or dipolar interactions can lead to increases in relaxation rates[44,45] and field-dependent pulse turning angles[46] relative to the isolated species. These differences can be exploited to separate the contributions of species using pulsed EPR spectra,[47] including echo detected spectra.[48-50] The ED spectrum is shown as a derivative in Figure 2 and gives component 1 characteristics but without the added features assigned

to the strongly dipolar coupled spectrum. This finding supports the assignment of a superposition spectrum for PrP(23−28, 57−91).

Strong dipolar coupling should be accompanied by a half field transition arising from a $\Delta M_s = 2$ transition.[51,52] Investigation of PrP(23−28, 57−91) in the vicinity of 1600 G indeed reveals a half field signal that is not observed in the monomeric octarepeats as shown in Figure 2.

To extract distance information, we performed simulations of both the full field $g \approx 2$ spectrum and the half field spectrum. The $g \approx 2$ spectrum was treated as a superposition, and the best fit suggested that the coupled spectrum comprised approximately 20% of the total signal with a distance between copper centers of 6.0 Å. The half field signal reveals a multiplet structure arising from the copper hyperfine interactions. Interestingly, at high copper occupancy, the half field signal persists but the muliplet lines are no longer resolved (data not shown). This is presumably due to interactions among more than two copper centers, thus giving rise to a superposition of multiplets with different hyperfine patterns. Two equivalents of copper gave the cleanest half field signal, and simulations were performed on this spectrum, as shown in Figure 2. Treating this spectrum as arising from a single coupled species, the best fit gave a distance of 4.9 Å. As a second approach for evaluating distances between copper centers, we examined the relative integrated intensities of the half field and $g \approx 2$ spectra. It is well established that this ratio scales as $1/r^6$.[51,52] Estimating that the coupled spectrum at $g \approx 2$ comprises approximately 20% of the total signal intensity, the distance determined by this approach gives approximately 3.5 Å. There may be a distribution of distances between copper centers. The $1/r^6$ dependence of the half field signal intensity, as compared to the $1/r^3$ dependence for the $g \approx 2$ dipolar coupling, gives a bias toward shorter distances,[52] and, hence, the value of 3.5 Å should be considered a lower bound.

These findings suggest a previously unseen packing interaction between copper binding segments in the component 1 coordination mode. The possible consequences of this interaction will be considered in the Discussion.

Journal of the American Chemical Society, Vol 127, No. 36 (September 14, 2005): pg. 12647-12656. DOI.

Component 2 Coordination – Intermediate Cu^{2+} Occupancy. Table 1 shows that component 2 binding is observed only in PrP constructs containing two or more octarepeat segments. Interestingly, the shortest PrP segment containing two HGGGW binding units, HGGGWGQPHGGGW, exhibits component 1 and component 2 spectra, but not component 3 (Supporting Information). Unfortunately, under all conditions studied, this construct gives a superposition of the two binding modes, thus confounding attempts to clearly characterize the molecular features exclusive to component 2.

Given that two sequential octarepeats provide a minimal model for component 2 binding, we sought an approach for blocking the formation of component 1. Component 1 binding arises from coordination of the His imidazole and deprotonated amide nitrogens from the two Gly residues immediately following the His (vide supra; also see Figure 6). Thus, *N*-methylation of either of these Gly residues to give the sarcosyl derivative of glycine will directly interfere with component 1 formation. This is investigated in Figure 3. Indeed, the construct HGXGWGQPHGXGW, where X = Sar (*N*-methyl glycine), when loaded with Cu^{2+} yields a spectrum with $g_{\|}$ and $A_{\|}$, and overall spectral shape equivalent to component 2. Moreover, the spectrum represents a homogeneous coordination environment with no indication of component 1 or other species. Blocking component 1 binding in an analogue of the full octarepeat domain using the construct KKRPKPWGQ(PHGXGWGQ)$_4$ gives a superposition of component 2 and component 3 (Supporting Information).

Journal of the American Chemical Society, Vol 127, No. 36 (September 14, 2005): pg. 12647-12656. DOI.

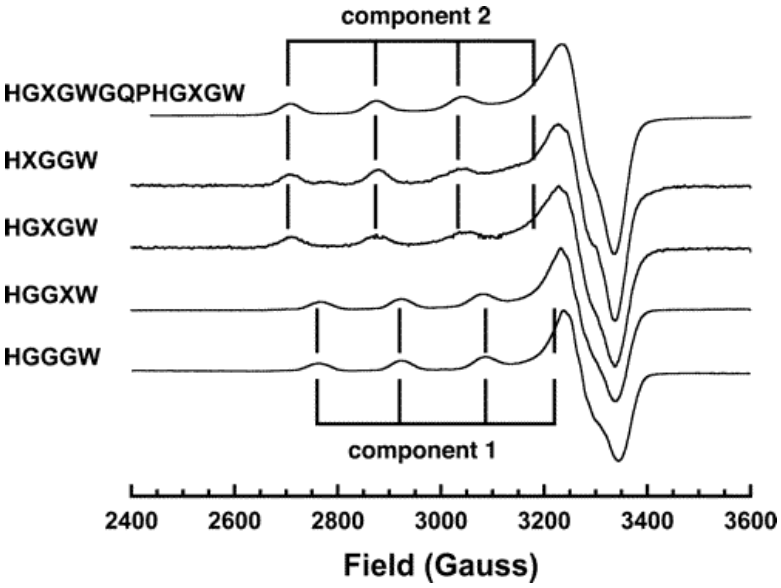

Figure 3 X-band EPR spectra of PrP constructs containing *N*-methylated glycine (sarcosine, X) at specific positions to block component 1 binding. Methylation of the first or second glycine results in pure component 2 binding.

Analysis of $g_{\parallel}$ and $A_{\parallel}$ of copper bound to HGXGWGQPHGXGW, as interpreted through the Peisach−Blumberg correlations,[43] suggests coordination by approximately two nitrogens and two oxygens (2N 2O), for an uncharged complex, or 3N 1O for a complex with a positive charge. To determine whether component 2 requires the two tandem octarepeats, the peptides HXGGW and HGXGW, derived from single repeats, were each independently investigated. Figure 3 shows that each of these peptides gives component 2 binding indistinguishable from that obtained from the two repeat construct HGXGWGQPHGXGW, although HXGGW does exhibit a weak signal at 2780 G that may represent an additional species. Methylation at the third glycine, which does not coordinate Cu^{2+} in component 1,[10] gives an EPR spectrum equivalent to unmodified HGGGW, as expected (Figure 3).

Three-pulse electron spin−echo envelope modulation (ESEEM) was performed to evaluate nearby, noncoordinated nitrogen atoms. With imidazole coordination, the remote nitrogen is ESEEM active and, indeed, serves as a diagnostic for equatorial binding of the His side chain.[53] In addition, for component 1, the nitrogen of the third Gly in the HGGGW sequence is also observable because it is rigidly held approximately 4 Å from the Cu^{2+} center by coordination of the amide carbonyl between the second and third Gly residues (see Figure 6).[10]

Journal of the American Chemical Society, Vol 127, No. 36 (September 14, 2005): pg. 12647-12656. DOI.

ESEEM spectra for HGXGWGQPHGXGW and HGXGW are shown in Figure 4. The spectra are approximately equivalent and give three low-frequency lines at 0.65, 0.85, and 1.50 MHz arising from transitions of a coupled ^{14}N in an electron spin manifold under near exact cancellation conditions, which is typical of imidazole coordination.[53,54] The broad signal near 4.0 MHz arises from the $\Delta m_I = 2$ transition from the other electron spin manifold. The ESEEM spectra suggest a Cu^{2+} center coordinated by a single equatorial imidazole. There is no evidence of either combination lines or an enhanced $\Delta m_I = 2$ transition as might be seen as arising from multiple imidazole coordination.[55] Moreover, direct simulations in the time domain (not shown) are fully consistent with a single equatorial imidazole.

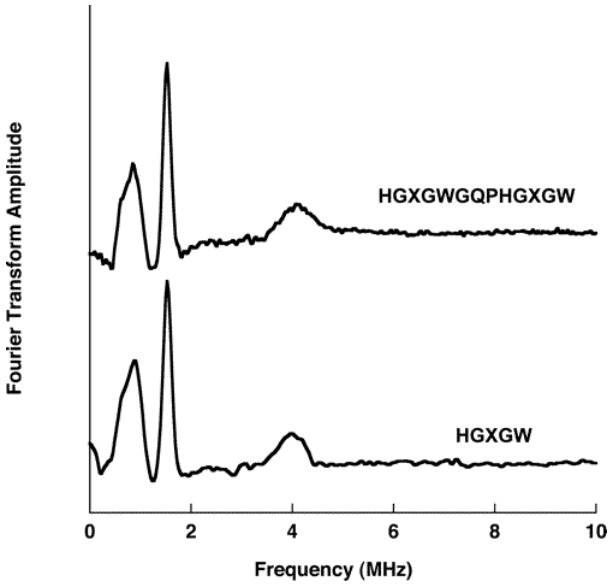

Figure 4 Three-pulse ESEEM spectra of constructs that exhibit component 2 binding showing single imidazole coordination. Spectra were obtained at 4.2 K from the $g_\perp$ region of the spectrum with τ = 150 ns.

Analysis of hyperfine multiplets arising from nitrogen couplings allows for direct mapping of the copper coordination environment. S-band EPR is ideal for resolving such couplings[56] and was used previously to identify nitrogens bound to copper in the octarepeat.[8,10] The benefit of S-band EPR arises from a partial cancellation of *g*-strain and *A*-strain induced inhomogeneous broadening specifically for the ^{63}Cu $m_I = -1/2$ hyperfine line.[56] HGXGW is chosen as a representative construct because it is the minimal peptide that gives a pure component 2 spectrum. The full S-band spectrum is shown in Figure 5

Journal of the American Chemical Society, Vol 127, No. 36 (September 14, 2005): pg. 12647-12656. DOI.

and indeed reveals superhyperfine couplings in the $m_I = -1/2$ line. The $m_I = -1/2$ line is further expanded in Figure 5B and reveals a five-line multiplet consistent with coordination by two nitrogens. To evaluate whether either of the Gly residues following the His coordinates to the copper center, ^{15}N-Gly analogues at the nonmethylated positons of of HGXGW were examined. A difference in multiplet structure upon change of nuclear spin ($I = 1$ for ^{14}N and $I = 1/2$ for ^{15}N) is directly observable if the modified nitrogen is equatorially bound to Cu^{2+}.[10] Figure 5 shows that there is no resolvable difference in the hyperfine pattern of the $m_I = -1/2$ line, demonstrating that neither of the labeled Gly residues are directly bound to the Cu^{2+} center.

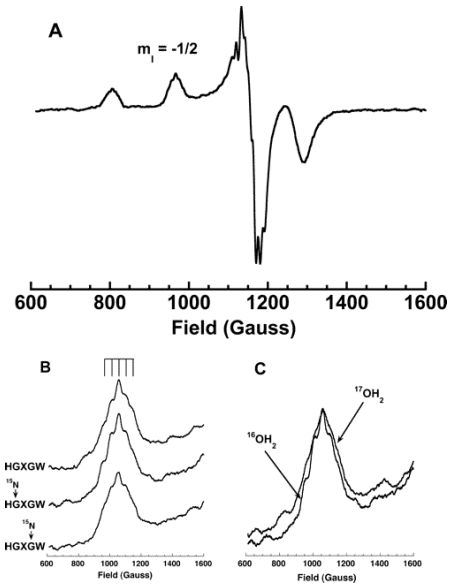

Figure 5 S-band EPR of HGXGW that favors component 2 binding. (A) Shows the full scan, (B) expansion of the $m_I = -1/2$ line, and (C) the $m_I = -1/2$ line from a sample containing 30% $^{17}OH_2$. The five line multiplet at $m_I = -1/2$ is consistent with coordination of two nitrogens. Insensitivity to ^{15}N placement at the first and third glycines shows that these residues do not coordinate. Broadening by $^{17}OH_2$ suggests that water contributes to the coordination sphere. Spectra (3.5 GHz) were acquired in D_2O solution at 133 K.

Histidine residues may coordinate through both the imidazole as well as the exocyclic backbone nitrogen. To test for this possibility in component 2, the peptide me-HGXGW was investigated. (We note that in addition to methylation, selectively ^{15}N labeled histidine would also be useful but is cost prohibitive.) Here, both the His backbone nitrogen as well as the second Gly were methylated. With standard acetylation of the N-terminus (see Materials and Methods), methylation at the His

Journal of the American Chemical Society, Vol 127, No. 36 (September 14, 2005): pg. 12647-12656. DOI.

exocyclic nitrogen removes any possibility of its coordination to copper. The observed X-band spectrum from a 1:1 complex of this peptide with Cu^{2+} is distinct from spectra observed for component 1, 2, or 3 binding (data not shown), thus demonstrating that His acts as a bidentate ligand for copper in component 2 binding.

The results above suggest that component 2 arises from copper coordination by both the His imidazole and its exocyclic nitrogen. As noted above, oxygen atoms likely occupy the remaining equatorial sites. To determine whether these oxygens are from solvent water molecules, EPR experiments were performed on HGXGW in ~30% ^{17}O water. The superhyperfine interaction of the ^{17}O nucleus ($I = {}^5/_2$), when coordinated to copper, usually results in line broadening.[57] At X-band, there was no appreciable difference in line shape. However, at S-band, broadening of the $m_I = -{}^1/_2$ line was clear as shown in Figure 5C, thus demonstrating the equatorial involvement of water. Preliminary simulations were used to determine whether the broadening was consistent with one or two water molecules, but the results were inconclusive.

The investigations above show that in component 2 copper binding, the octarepeat His provides two equatorial nitrogens with water at one or both of the remaining equatorial sites resulting in 2N 2O coordination, as shown in Figure 6. His acts as a bidentate ligand forming a six-membered ring with Cu^{2+} as found in crystal structures of Cu−His complexes.[58,59] This coordination mode is fully consistent with the X- and S-band EPR, as well as the ESEEM studies on the methylated and isotopically labeled peptides examined here.

Journal of the American Chemical Society, Vol 127, No. 36 (September 14, 2005): pg. 12647-12656. DOI.

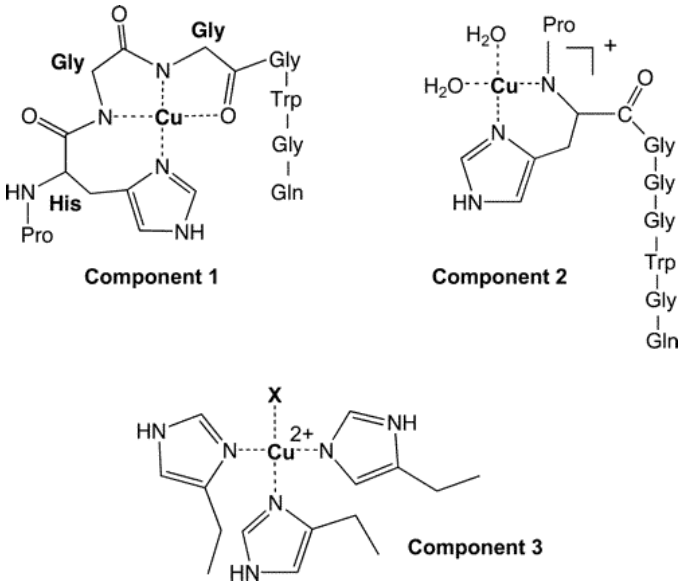

Figure 6 Models of the three equatorial coordination modes. For component 3, X may represent either a fourth imidazole or a water molecule.

Because the proposed component 2 coordination mode (Figure 6) appears to take up all of the equatorial sites, Cu^{2+} should form a 1:1 complex with each octarepeat His. To test this directly, EPR detected titrations were performed on HGXGWGQPHGXGW and HGXGW using previously established methods.[8,11] The longer peptide with two putative binding segments takes up between 1.0 and 1.5 copper ions, and the pentamer binds as a 2:1 complex with copper. In contrast to the expected 1:1 stoichiometry, these data suggest that two HGGGW segments are required to stabilize component 2 binding. To determine whether a neighboring His makes an additional contact with Cu^{2+}, we examined the His → Tyr substituted constructs HGGGWGQPYGGGW and YGGGWGQPHGGGW, as well as an analogue with three linked HGGGW segments, but with a His → Tyr mutation at the second repeat (Table 1). Tyrosine was chosen because it is approximately equivalent to His in size, is reasonably soluble, but lacks a nitrogen capable of coordinating copper. Interestingly, all of these constructs exhibit exclusively component 1 binding, as determined by X-band EPR (data not shown).

The ESEEM spectra are consistent with a single equatorial imidazole, and the five-line $m_I = -1/2$ multiplet in the S-band spectra indicates only two equatorial nitrogens. However, binding stoichiometry and constructs with His → Tyr mutations suggest that

Journal of the American Chemical Society, Vol 127, No. 36 (September 14, 2005): pg. 12647-12656. DOI.

two His residues in sequential repeat segments are required to stabilize component 2. These data argue that a second imidazole may coordinate but in an axial position. In square-pyramidal coordination geometry, axial bonds to Cu^{2+} are often much longer and weaker than equatorial due to the Jahn−Teller distortion. Although EPR spectra are usually not sensitive to axial nitrogens, they may under some circumstances be detectable by ESEEM arising from the directly bound ^{14}N.[39] However, this signal is weak and typically not visible in the presence of strong ESEEM signals from an equatorial imidazole.[60] The likelihood of this coordination mode and its structural implications will be considered in the Discussion.

Component 3 Coordination − Low Cu^{2+} Occupancy. Component 3 coordination is observed only in the constructs KKRPKPWGQ(PHGGGWGQ)$_4$, KKRPKPWGQ(PHGXGWGQ)$_4$, and (PHGGGWGQ)$_3$ at low copper load (<1.0 equiv), and thus requires three or four sequential HGGGW segments. Analysis of $g_\parallel$ and $A_\parallel$ suggests 3N 1O or 4N coordination (Table 2). In addition, reduction of pH to 6.5, at a fixed Cu^{2+} concentration, leads to a relative loss of component 1 binding but does not influence component 3 (data not shown). The accumulation of these observations suggests that component 3 arises from coordination of three or four neutral imidazoles and is likely the dominant species previously observed at reduced pH.[8,25] In support of this assignment, Cu^{2+} in a 50-fold molar excess of imidazole gives a spectrum that is nearly indistinguishable from that of component 3 (data not shown), and the coupling terms $g_\parallel$ and $A_\parallel$ (Table 2) are close to those reported by Malmstrom and Vanngard from Cu^{2+} with excess imidazole at pH 6.8.[61]

ESEEM is sensitive to multiple imidazole coordination as reflected through combination peaks and an enhanced $\Delta m_I = 2$ signal.[55] ESEEM spectra for PrP(23−28, 57−91) with 1.0 and 4.0 equiv of Cu^{2+} are shown in Figure 7. The spectrum at 4.0 equiv (component 1) was previously assigned using ^{15}N labeling and two-dimensional hyperfine sublevel correlation spectroscopy (HYSCORE) and arises from the His imidazole and the amide nitrogen of the third Gly in the HGGGW segment.[10] This spectrum shows no indication of combination peaks, and the $\Delta m_I = 2$ signal at approximately 4.0 MHz is consistent with a single imidazole. At 1.0 equiv, however, there are marked

Journal of the American Chemical Society, Vol 127, No. 36 (September 14, 2005): pg. 12647-12656. DOI.

changes in the ESEEM spectrum (Figure 7). The lines arising from the noncoordinated Gly(3) amide nitrogen are lost. Most notably, the $\Delta m_I = 2$ signal is now prominent and, relative to the intense peak at 1.5 MHz, is increased in amplitude by a factor of 2−3 over that obtained with 4.0 equiv of Cu^{2+}. There are also weak signals at approximately 2.1, 2.4, and 3.1 MHz, consistent with combination peaks arising from the fundamental low-frequency lines at exact cancellation. S-band EPR was also obtained from PrP(23−28, 57−91) with 1.0 equiv of copper and revealed a well-resolved seven- or nine-line multiplet for the $m_I = -1/2$ line (inset) consistent with coordination by three or four equivalent nitrogens. Together, these data clearly suggest that component 3 arises from multiple imidazole coordination.

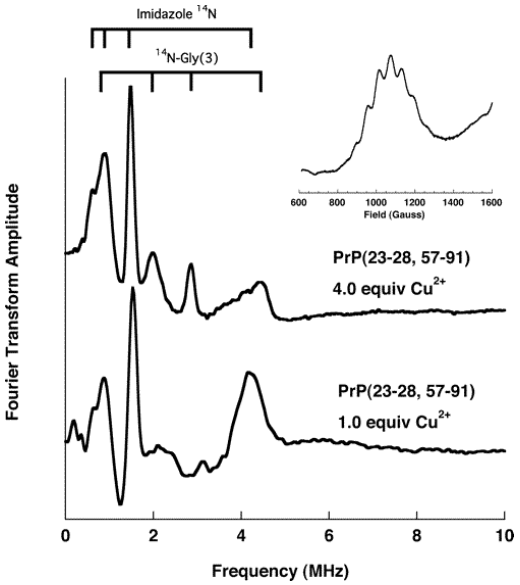

Figure 7 Three-pulse ESEEM comparing PrP(23−28, 57−91) with 4.0 and 1.0 equiv of Cu^{2+}. At 4.0 equiv, component 1 dominates; the grid at the top shows the previously determined assignment.[10] At 1.0 equiv, which favors component 3, the enhanced $\Delta m_I = 2$ feature at 4.1 MHz is consistent with multiple His coordination. The inset shows the S-band $m_I = -1/2$ line obtained with 1.0 equiv. The seven- or nine-line pattern suggests 3N1O or 4N coordination by equivalent nitrogens.

To gain insight into the three-dimensional characteristics of the distinct copper binding components, structural calculations were performed using distance restraints arising from coordination sphere appropriate for each of the binding modes. The polypeptide backbone was left unrestrained, except where noted, thus resulting in significant variations in backbone geometry for intervening loops. The results are shown in Figure 8. Component 3 was calculated with coordination from

Journal of the American Chemical Society, Vol 127, No. 36 (September 14, 2005): pg. 12647-12656. DOI.

the three N-terminal, octarepeat His imidazoles (His60, His68, His76), with the fourth octarepeat His (residue 84) left free. The resulting structure reveals an extensive segment of disordered polypeptide of approximately 40 amino acids between the last His of the copper binding segment (in this three His coordination structure) and the first β-strand of the globular domain. Component 2 was developed using the equatorial coordination mode shown in Figure 6 and an additional long copper bond (2.4 Å) to the adjacent His imidazole in the following octapeptide segment. The structure gives rise to two rather large loops, each closed by copper coordination. Component 1 was developed using the known restraints from the crystal structure of Cu^{2+}-HGGGW. In addition to extensive copper contacts to the His, Gly, and Trp residues, two copper ions in adjacent repeats were brought into close proximity of approximately 4.0 Å based on the observed dipolar couplings.

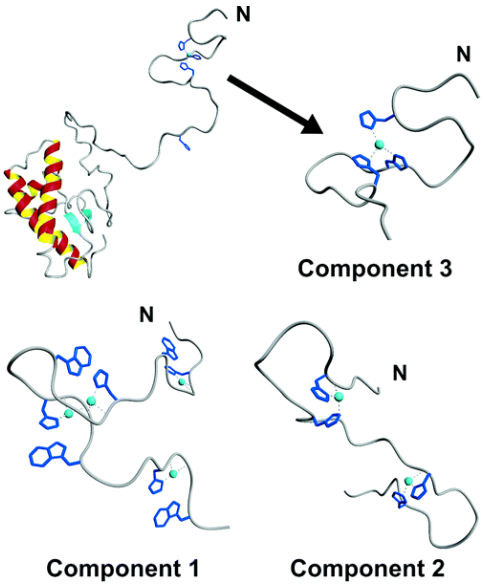

Figure 8 Models of PrP^C containing Cu^{2+} in the three coordination modes. The figure at upper left shows PrP(60−231) bound to a single Cu^{2+} with component 3 coordination. To the upper right, the copper binding octarepeat domain is expanded. In this mode, an additional His imidazole may also participate in copper binding. For components 1 and 2, only the octarepeat domains are shown.

Discussion

The octarepeat domain of PrP, at pH 7.4, passes through a series of distinct binding modes as a function of Cu^{2+} concentration. The equatorial features are summarized in Figure 6, and

Journal of the American Chemical Society, Vol 127, No. 36 (September 14, 2005): pg. 12647-12656. DOI.

representative N-terminal structures are shown in Figure 8. At low occupancy, less than 1 equiv of Cu^{2+}, three or four His imidazoles from adjacent octarepeat segments contribute to the coordination sphere (component 3 binding). This binding mode persists at a reduced pH of 6.5. Between 1 and 2 equiv, individual histidines provide the equatorial environment, binding through the imidazole and the deprotonated exocyclic nitrogen. The overall charge at the component 2 center is +1 resulting from the +2 charge of the copper and the −1 charge of the histidine backbone amide nitrogen. Water molecules also contribute to the coordination sphere. A second imidazole is also implicated in component 2 binding; however, this interaction is not reflected by ESEEM studies. Finally, from 2 to 4 equiv, where the octarepeat domain saturates with Cu^{2+}, component 1 coordination dominates. This mode, described previously by both EPR and X-ray crystallography,[10] yields a neutral copper center because the charge on the metal ion is offset by the two negative charges from the sequential deprotonated glycine amides. Dipolar couplings and half field EPR signals indicate that component 1 is accompanied by a significant population of copper centers in near proximity, separated by 3.5−6 Å.

The data presented herein, along with previous studies, provide a clear picture of both component 1 and component 3 binding. Component 2, however, remains enigmatic. EPR spectra obtained from various peptide constructs suggest that two adjacent octarepeats are required to stabilize component 2. Substitution of His with Tyr in either of the adjacent octapeptide repeats eliminates the component 2 signal. Although these data suggest that two imidazoles coordinate to a single Cu^{2+} center, this is not supported by ESEEM, which gives the characteristic signal of a single equatorial imidazole. To reconcile these findings, we consider two possibilities. First, the peptide conformation may control the component 1/component 2 equilibrium. As noted, two adjacent octarepeats are sufficient for both binding modes, with component 1 dominating at full occupancy (2 equiv − one copper per octarepeat). At half occupancy, with a single Cu^{2+} or less, the peptide may be structured in a fashion that competes against normal component 1 binding. For example, in interleukin-6, nuclear magnetic resonance (NMR) shows that the side chains pairs Trp and His interact, thus stabilizing secondary structure.[62] Considering only two adjacent octarepeats, it is noted that the segment WGQPH separates the glycine

Journal of the American Chemical Society, Vol 127, No. 36 (September 14, 2005): pg. 12647-12656. DOI.

triplets. Perhaps an interaction between Trp and His stabilizes a β-turn. Without the Trp indole available for component 1 coordination, the copper may be driven instead to the remaining N-terminal His in a component 2 binding fashion. Recent NMR experiments on HGGGWGQP and $(HGGGQGQP)_3$ in the absence of copper indeed do find evidence of turns involving Trp.[63] However, these studies also find that the HGGGW segment adopts a conformation similar to that involved in component 1 binding. In contrast to peptide conformation competing with component 1 binding, it appears that the octarepeat domain actually preorganizes to stabilize this binding mode.

A second possible role for the additional His in component 2 binding is direct imidazole coordination but through a longer and weaker copper−nitrogen bond. Here, two recent crystallographic studies are instructive. The complex $Cu(His)_2$ is relevant both as a source of exchangeable Cu^{2+} in blood and also as a means of delivering therapeutic levels of copper in Menkes disease.[64] One might expect this complex to organize in a symmetric fashion with both histidines contributing equally to the coordination environment. Indeed, the complex Cu(d-His)(l-His) forms a structure in which each His coordinates through an imidazole nitrogen and amino nitrogen,[58] very much like component 2. Just recently, the $Cu(l\text{-}His)_2$ structure was determined and, surprisingly, revealed crystallographically distinct histidine coordination.[59] In the equatorial plane, one His bound through its imidazole and amino nitrogens, whereas the other His bound through its amino nitrogen and carboxylate oxygen. An equivalent coordination mode had been previously determined from ESEEM investigations on copper-doped single crystals of l-histidine.[65] From a structural perspective, these studies may suggest that when an l-His coordinates through its two nitrogens, steric constraints may interfere with coordination of a second equatorial imidazole (although we do note that a recent high field electron nuclear double resonance (ENDOR) study did identify a symmetric bis-His copper complex with each His contributing amino and imidazole nitrogens[66]). An unusual bis-His complex was recently elucidated in a mutant of nitrite reductase.[67] In the wild-type protein, the type 2 Cu^{2+} center involves three imidazoles. Removal of one of the imidazole groups in an H/V mutant results in a bis-His complex with a water molecule contributing to the coordination environment. Interestingly, the imidazoles are

Journal of the American Chemical Society, Vol 127, No. 36 (September 14, 2005): pg. 12647-12656. DOI.

inequivalent with respect to the copper−nitrogen bond length. One bond is approximately 2.0 Å, whereas the other is approximately 2.4 Å. The shorter bond length is typical of equatorial coordination, whereas the longer bond is reminiscent of axial coordination in Cu^{2+} centers. As noted in the Results section, ESEEM of longer axial bonds is extremely weak and difficult to observe in the presence of equatorial imidazole coordination.[60] In light of these findings, we propose that component 2 likely involves two imidazoles at the copper center but with one in an axial position that is relatively ESEEM silent.

Our studies presented here link well with several recent investigations into PrP-copper binding. Valensin et al. reported detailed potentiometric titrations on $(PHGGGWGQ)_2$ and $(PHGGGWGQ)_4$.[34] At fixed copper/peptide ratios, pH is scanned while monitoring proton release. Remarkably, these investigations reveal a wide range of distinct deprotonated species. Focusing on their data obtained with 1.0 equiv of copper interacting with $(PHGGGWGQ)_4$ at pH 7.4, they find evidence for a dominant species that has retained its backbone protons, consistent with component 3. With 4.0 copper equiv, the principle species just above pH 7.0 has given up nine protons. Our component 1 binding mode (Figure 6) requires a loss of two protons per bound Cu^{2+}, which is quite close to that identified by Valensin et al. They did not examine $(PHGGGWGQ)_4$ with 2.0 equiv of Cu^{2+}. However, just above pH 6.0, they do find a species that has given up one proton for each bound copper, consistent with component 2. In this same study, NMR results obtained from $(PHGGGWGQ)_2$ with trace amounts of added Cu^{2+} show line broadening consistent with multiple His coordination, again consistent with the component 3 structure.

Morante et al. used extended X-ray absorption spectroscopy (XAS), both XANES and EXAFS, to probe copper binding in partially and fully occupied octarepeat constructs, as well as in bovine rPrP.[33] At full occupancy, their analysis supported our reported crystal structure with single imidazole coordination. However, at partial occupancy, additional spectral features were identified consistent with two coordinated imidazoles. These results held for octarepeat peptides as well as full-length rPrP. On the basis of fluorescence titrations, Jackson et al. suggested that the full PrP octarepeat domain binds only a single Cu^{2+} with high affinity.[15] Although the reported affinities from this

Journal of the American Chemical Society, Vol 127, No. 36 (September 14, 2005): pg. 12647-12656. DOI.

study have been questioned,[32] their modeling studies nevertheless revealed low energy conformations with four-imidazole coordination. Together, these disparate studies clearly point to diverse binding modes, as directly observed here.

With regard to component 1 binding, our studies reveal dipolar couplings arising from proximal copper centers. The dipolar signal grows in concomitantly with component 1 formation and, therefore, most likely arises from packing interactions between the structured Cu^{2+}-HGGGW segments. As noted in the Results section, analysis of the dipolar splitting versus the half field signal intensity yields different distance measurements, most likely indicating a range of copper−copper distances. Direct interpretation of these data is difficult because the observed distance-dependent signals may arise from the interaction of more than two copper centers. Nevertheless, the short 3.0−6.0 Å distance range (Results) suggests that the individual component 1 segments come into van der Waals contact. (Note that the axial bond to water is approximately 2.4 Å so that stacking of the ordered Cu^{2+}-HGGGW segments would place the copper centers approximately 3.0 Å apart.) Individual component 1 sites are uncharged, as are the intervening GQP linker segments. Consequently, upon full copper occupancy, the coupling data observed here suggest that the octarepeat domain undergoes a partial hydrophobic collapse. Such a collapse, similar to the principle force of protein folding, may be mechanistically important. Using circular dichroism (CD) and binding competition studies, Garnett and Viles found that the octarepeat domain binds copper with strong positive cooperativity, accompanied by structural organization of the GQP linker (Table 1) between Cu^{2+}-HGGGW segments.[32] However, cooperative binding was not observed for constructs containing only one or two octarepeats. It was argued that at full copper occupancy, the octarepeat domain takes on structure. Our results are consistent with this proposal and suggest a physical driving force underlying structural reorganization upon full copper occupancy.

The function of PrP^C remains unknown. PrP^C is internalized by endocytosis at high copper concentrations, suggesting that PrP may function as a copper sensor or transporter.[27] The significant structural changes associated with the transition from component 3 to

Journal of the American Chemical Society, Vol 127, No. 36 (September 14, 2005): pg. 12647-12656. DOI.

component 1 binding (Figure 8) may serve to transduce the signal for this internalization process. Although copper-induced endocytosis is well established, it is not yet clear how this process links to any specific PrP^C function.[28,68] Nevertheless, the emerging consensus is that PrP^C plays a neuroprotective role.[69] Several mechanisms of action have been proposed including cell signaling, suppression of apoptosis, and antioxidant activity.[69] With regard to antioxidant function, it has been argued that PrP^C is an enzyme – a neuronal superoxide dismutase (SOD).[70,71] However, the relatively weak micromolar affinity observed for Cu^{2+} association with PrP is not characteristic of known SODs.[31,32] In addition, assays aimed at evaluating SOD function in brain tissue as a function of PrP expression failed to find enhanced activity.[68,72] Here, we show that the octarepeat domain takes on widely varying structures as a function of copper load. This is also uncharacteristic of known SODs and, in accord, argues against such function.

With regard to a neuroprotective role, several lines of investigation do suggest an intimate relationship between PrP and localized copper concentrations. Within the central nervous system, PrP^C is concentrated at presynaptic membranes.[4] There is significant copper efflux into the synapse as a function of both exocytosis and neuronal depolarization.[73-75] The peak synaptic concentration is not certain, but estimates place $[Cu^{2+}]$ within the range from 3.0 μM[74] to 250 μM.[75] It appears that copper efflux is an obligatory component of vesicle fusion leading to the release of neurotransmitter.[5] Yet, experiments using cell culture demonstrate that copper concentrations in excess of 10 μM are toxic to neurons.[76] Of significance here, PrP is able to ameliorate this toxic effect – the protein binds Cu^{2+} at the plasma membrane,[28] and wild-type cells are more resistant to copper-mediated oxidative stress as compared to PrP knockouts.[28,76]

Recent work with the doppel protein also supports a neuroprotective role for PrP. The doppel protein is structurally homologous to the globular C-terminus of PrP but lacks the PrP N-terminal octarepeat domain.[77] Doppel protein (Dpl) is normally expressed in the testis.[77] However, work with transgenic mice has shown that expression of Dpl in the central nervous system leads to apoptosis and ataxia; this effect is offset by coexpression with PrP.

Journal of the American Chemical Society, Vol 127, No. 36 (September 14, 2005): pg. 12647-12656. DOI.

Interestingly, recent mutagenesis experiments have shown that PrP's ability to protect against Dpl toxicity requires the octarepeat domain.[78]

Given that PrP^C takes up 4 equiv of Cu^{2+} in the octarepeat domain, and that this domain is key for neuroprotection, points toward a different type of antioxidant function. Component 1 binding stabilizes copper in the Cu^{2+} oxidation state, thus reducing potential copper-mediated redox chemistry.[9] Thus, instead of acting as a redox enzyme, PrP^C may actually function as a copper buffer that sequesters the ion in a relatively redox inactive form.[5,17] In this scenario, the antioxidant character arises from protection against deleterious copper-mediated oxidation chemistry. Our structural studies here show that component 1 is dominant at high copper occupancy and thus maximizes PrP^C's antioxidant character with increasing Cu^{2+} concentrations.

The studies here provide structural details on the fundamental copper binding modes at pH 7.4. However, it is currently unknown which of the three modes are dominant in vivo. Moreover, it is not clear how the globular C-terminal domain, or its mutants, influences the equilibrium among these copper binding states. Elucidation of these issues is sure to provide important new insights into PrP^C function and how the formation of PrP^{Sc} contributes to loss of this function.

Acknowledgment

This work was supported by NIH grants GM 65790 (G.L.M.), GM 40168 (J.P.), GM 60609 (G.J.G.), and NSF instrumentation grant DBI-0217922 (G.L.M.).

Supporting Information Available

EPR spectra for various octarepeat constructs as a function of copper concentration. This material is available free of charge via the Internet at http://pubs.acs.org.

References

[1]Prusiner, S. B. *Proc. Natl. Acad. Sci. U.S.A.* **1998**, *95*, 13363−13383.
[2]Prusiner, S. B. *Science* **1997**, *278*, 245−251.
[3]Legname, G.; Baskakov, I. V.; Nguyen, H. O.; Riesner, D.; Cohen, F. E.; DeArmond, S. J.; Prusiner, S. B. *Science* **2004**, *305*, 673−6.

[4]Herms, J.; Tings, T.; Gall, S.; Madlung, A.; Giese, A.; Siebert, H.; Schürmann, P.; Windl, O.; Brose, N.; Kretzschmar, H. *J. Neurosci.* **1999**, *19*, 8866−8875.

[5]Vassallo, N.; Herms, J. *J. Neurochem.* **2003**, *86*, 538−44.

[6]Caughey, B.; Chesebro, B. *Trends Cell Biol.* **1997**, *7*, 56−62.

[7]Brown, D. R.; Qin, K.; Herms, J. W.; Madlung, A.; Manson, J.; Strome, R.; Fraser, P. E.; Kruck, T.; von Bohlen, A.; Schulz-Schaeffer, W.; Giese, A.; Westway, D.; Kretzschmar, H. *Nature* **1997**, *390*, 684−687.

[8]Aronoff-Spencer, E.; Burns, C. S.; Avdievich, N. I.; Gerfen, G. J.; Peisach, J.; E., A. W.; Ball, H. L.; Cohen, F. E.; Prusiner, S. B.; Millhauser, G. L. *Biochemistry* **2000**, *39*, 13760−13771.

[9]Bonomo, R. P.; Impellizzeri, G.; Pappalardo, G.; Rizzarelli, E.; Tabbi, G. *Chem.-Eur. J.* **2000**, *6*, 4195−4202.

[10]Burns, C. S.; Aronoff-Spencer, E.; Dunham, C. M.; Lario, P.; Avdievich, N. I.; Antholine, W. E.; Olmstead, M. M.; Vrielink, A.; Gerfen, G. J.; Peisach, J.; Scott, W. G.; Millhauser, G. L. *Biochemistry* **2002**, *41*, 3991−4001.

[11]Burns, C. S.; Aronoff-Spencer, E.; Legname, G.; Prusiner, S. B.; Antholine, W. E.; Gerfen, G. J.; Peisach, J.; Millhauser, G. L. *Biochemistry* **2003**, *42*, 6794−803.

[12]Hasnain, S. S.; Murphy, L. M.; Strange, R. W.; Grossmann, J. G.; Clarke, A. R.; Jackson, G. S.; Collinge, J. *J. Mol. Biol.* **2001**, *311*, 467−473.

[13]Hornshaw, M. P.; McDermott, J. R.; Candy, J. M. *Biochem. Biophys. Res. Commun.* **1995**, *207*, 621−629.

[14]Hornshaw, M. P.; McDermott, J. R.; Candy, J. M.; Lakey, J. H. *Biochem. Biophys. Res. Commun.* **1995**, *214*, 993−9.

[15]Jackson, G. S.; Murray, I.; Hosszu, L. L. P.; Gibbs, N.; Waltho, J. P.; Clarke, A. R.; Collinge, J. *Proc. Natl. Acad. Sci. U.S.A.* **2001**, *98*, 8531−8535.

[16]Jones, C. E.; Klewpatinond, M.; Abdelraheim, S. R.; Brown, D. R.; Viles, J. H. *J. Mol. Biol.* **2005**, *346*, 1393−407.

[17]Millhauser, G. L. *Acc. Chem. Res.* **2004**, *37*, 79−85.

[18]Miura, T.; Hori-i, A.; Mototani, H.; Takeuchi, H. *Biochemistry* **1999**, *38*, 11560−11569.

[19]Pushie, M. J.; Rauk, A. *J. Biol. Inorg. Chem.* **2003**, *8*, 53−65.

[20]Qin, K.; Yang, Y.; Mastrangelo, P.; Westaway, D. *J. Biol. Chem.* **2002**, *277*, 1981−1990.

[21]Stöckel, J.; Safar, J.; Wallace, A. C.; Cohen, F. E.; Prusiner, S. B. *Biochemistry* **1998**, *37*, 7185−7193.

[22]Van Doorslaer, S.; Cereghetti, G. M.; Glockshuber, R.; Schweiger, A. *J. Phys. Chem.* **2001**, *105*, 1631−1639.

[23]Whittal, R. M.; Ball, H. L.; Cohen, F. E.; Burlingame, A. L.; Prusiner, S. B.; Baldwin, M. A. *Protein Sci.* **2000**, *9*, 332−343.

Journal of the American Chemical Society, Vol 127, No. 36 (September 14, 2005): pg. 12647-12656. DOI.

[24]Cereghetti, G. M.; Schweiger, A.; Glockshuber, R.; Van Doorslaer, S. *Biophys. J.* **2003**, *84*, 1985−97.
[25]Miura, T.; Sasaki, S.; Toyama, A.; Takeuchi, H. *Biochemistry* **2005**, *44*, 8712−20.
[26]Donne, D. G.; Viles, J. H.; Groth, D.; Mehlhorn, I.; James, T. L.; Cohen, F. E.; Prusiner, S. B.; Wright, P. E.; Dyson, H. J. *Proc. Natl. Acad. Sci. U.S.A.* **1997**, *94*, 13452−13456.
[27]Pauly, P. C.; Harris, D. A. *J. Biol. Chem.* **1998**, *273*, 33107−33119.
[28]Rachidi, W.; Vilette, D.; Guiraud, P.; Arlotto, M.; Riondel, J.; Laude, H.; Lehmann, S.; Favier, A. *J. Biol. Chem.* **2003**, *278*, 9064−9072.
[29]Zeng, F.; Watt, N. T.; Walmsley, A. R.; Hooper, N. M. *J. Neurochem.* **2003**, *84*, 480−90.
[30]Klamt, F.; Dal-Pizzol, F.; Conte DA Frota, M. L., Jr.; Walz, R.; Andrades, M. E.; Gomes DA Silva, E.; Brentani, R. R.; Izquierdo, I.; Moreira, J. C. F. *Free Radical Biol. Med.* **2001**, *30*, 1137−1144.
[31]Kramer, M. L.; Kratzin, H. D.; Schmidt, B.; Romer, A.; Windl, O.; Liemann, S.; Hornemann, S.; Kretzschmar, H. *J. Biol. Chem.* **2001**, *276*, 16711−16719.
[32]Garnett, A. P.; Viles, J. H. *J. Biol. Chem.* **2003**, *278*, 6795−802.
[33]Morante, S.; Gonzalez-Iglesias, R.; Potrich, C.; Meneghini, C.; Meyer-Klaucke, W.; Menestrina, G.; Gasset, M. *J. Biol. Chem.* **2004**, *279*, 11753−9.
[34]Valensin, D.; Luczkowski, M.; Mancini, F. M.; Legowska, A.; Gaggelli, E.; Valensin, G.; Rolka, K.; Kozlowski, H. *Dalton Trans.* **2004**, 1284−93.
[35]Zuckermann, R. N.; Kerr, J. M.; Kent, S. B. H.; Moos, W. H. *J. Am. Chem. Soc.* **1992**, *114*, 10646−10647.
[36]Miller, S. C.; Scanlan, T. S. *J. Am. Chem. Soc.* **1997**, *119*, 2301−2302.
[37]Jiang, F.; McCraken, J.; Peisach, J. *J. Am. Chem. Soc.* **1990**, *112*, 9035−9044.
[38]Bender, C. J.; Casimiro, D. R.; Peisach, J.; Dyson, H. J. *J. Chem. Soc., Faraday Trans.* **1997**, *93*, 3967−3980.
[39]Cornelius, J. B.; McCracken, J.; Clarkson, R. B.; Belford, R. L.; Peisach, J. *J. Phys. Chem.* **1990**, *94*, 6977−6982.
[40]Bennett, B.; Antholine, W. E.; D'Souza V. M.; Chen, G.; Ustinyuk, L.; Holz, R. C. *J. Am. Chem. Soc.* **2002**, *124*, 13025−34.
[41]Hanson, G. R.; Gates, K. E.; Noble, C. J.; Griffin, M.; Mitchell, A.; Benson, S. *J. Inorg. Biochem.* **2004**, *98*, 903−16.
[42]Herrmann, T.; Guntert, P.; Wuthrich, K. *J. Mol. Biol.* **2002**, *319*, 209−27.
[43]Peisach, J.; Blumberg, W. E. *Arch. Biochem. Biophys.* **1974**, *165*, 691−708.
[44]Hirsh, D. J.; Beck, W. F.; Lynch, J. B.; Que, L.; Brudvig, G. W. *J. Am. Chem. Soc.* **1992**, *114*, 7475−7481.
[45]Seiter, M.; Budker, V.; Du, J. L.; Eaton, G. R.; Eaton, S. S. *Inorg. Chim. Acta* **1998**, *273*, 354−366.

Journal of the American Chemical Society, Vol 127, No. 36 (September 14, 2005): pg. 12647-12656. DOI.

[46]Eaton, S. S.; Eaton, G. R. *J. Magn. Reson., Ser. A* **1995**, *117*, 62−66.
[47]Maly, T.; MacMillan, F.; Zwicker, K.; Kashani-Poor, N.; Brandt, U.; Prisner, T. F. *Biochemistry* **2004**, *43*, 3969−78.
[48]Hoffmann, E.; Schweiger, A. *Appl. Magn. Reson.* **1995**, *9*, 1−22.
[49]Lawrence, C. C.; Bennati, M.; Obias, H. V.; Bar, G.; Griffin, R. G.; Stubbe, J. *Proc. Natl. Acad. Sci. U.S.A.* **1999**, *96*, 8979−8984.
[50]Mehring, M.; Seidel, H.; Muller, W.; Wegner, G. *Solid State Commun.* **1983**, *45*, 1075−1077.
[51]Eaton, S. S.; More, K. M.; Sawant, B. M.; Eaton, G. R. *J. Am. Chem. Soc.* **1983**, *105*, 6560−6567.
[52]Anderson, D. J.; Hanson, P.; McNulty, J.; Millhauser, G.; Monaco, V.; Formaggio, F.; Crisma, M.; Toniolo, C. *J. Am. Chem. Soc.* **1999**, *121*, 6919−6927.
[53]Mims, W. B.; Peisach, J. *J. Chem. Phys.* **1978**, *69*, 4921−4930.
[54]Flanagan, H. L.; Singel, D. J. *J. Chem. Phys.* **1987**, *87*, 5606−5616.
[55]Mccracken, J.; Pember, S.; Benkovic, S. J.; Villafranca, J. J.; Miller, R. J.; Peisach, J. *J. Am. Chem. Soc.* **1988**, *110*, 1069−1074.
[56]Froncisz, W.; Hyde, J. S. *J. Phys. Chem.* **1980**, *73*, 3123−3131.
[57]Deinum, J. S.; Vanngard, T. *FEBS Lett.* **1975**, *58*, 62−5.
[58]Camerman, N.; Fawcett, J. K.; Kruck, T. P. a.; Sarkar, B.; Camerman, a. *J. Am. Chem. Soc.* **1978**, *100*, 2690−2693.
[59]Deschamps, P.; Kulkarni, P. P.; Sarkar, B. *Inorg. Chem.* **2004**, *43*, 3338−40.
[60]Jiang, F.; Peisach, J.; Ming, L. J.; Que, L., Jr.; Chen, V. J. *Biochemistry* **1991**, *30*, 11437−45.
[61]Malmstrom, B. G.; Vanngard, T. *J. Mol. Biol.* **1960**, *2*, 118−124.
[62]Matthews, J. M.; Ward, L. D.; Hammacher, A.; Norton, R. S.; Simpson, R. J. *Biochemistry* **1997**, *36*, 6187−96.
[63]Zahn, R. *J. Mol. Biol.* **2003**, *334*, 477−88.
[64]DiDonato, M.; Sarkar, B. *Biochim. Biophys. Acta* **1997**, *1360*, 3−16.
[65]Colaneri, M. J.; Peisach, J. *J. Am. Chem. Soc.* **1992**, *114*, 5335−5341.
[66]Manikandan, P.; Epel, B.; Goldfarb, D. *Inorg. Chem.* **2001**, *40*, 781−7.
[67]Ellis, M. J.; Antonyuk, S. V.; Strange, R. W.; Sawers, G.; Eady, R. R.; Hasnain, S. S. *Inorg. Chem.* **2004**, *43*, 7591−3.
[68]Waggoner, D. J.; Drisaldi, B.; Bartnikas, T. B.; Casareno, R. L. B.; Prohaska, J. R.; Gitlin, J. D.; Harris, D. A. *J. Biol. Chem.* **2000**, *275*, 7455−7458.
[69]Roucou, X.; Gains, M.; LeBlanc, A. C. *J. Neurosci. Res.* **2004**, *75*, 153−61.
[70]Brown, D. R.; Wong, B.-S.; Hafiz, F.; Clive, C.; Haswell, S. J.; Jones, I. M. *Biochem. J.* **1999**, *344*, 1−5.
[71]Daniels, M.; Brown, D. R. *Methods Enzymol.* **2002**, *349*, 258−267.
[72]Hutter, G.; Heppner, F. L.; Aguzzi, A. *Biol. Chem.* **2003**, *384*, 1279−85.
[73]Hartter, D. E.; Barnea, A. *Synapse* **1988**, *2*, 412−5.

[74]Hopt, A.; Korte, S.; Fink, H.; Panne, U.; Niessner, R.; Jahn, R.; Kretzschmar, H.; Herms, J. *J. Neurosci. Methods* **2003**, *128*, 159−72.
[75]Kardos, J.; Kovacs, I.; Hajos, F.; Kalman, M.; Simonyi, M. *Neurosci. Lett.* **1989**, *103*, 139−44.
[76]Brown, D. R.; Schmidt, B.; Kretzschmar, H. A. *J. Neurochem.* **1998**, *70*, 1686−1693.
[77]Westaway, D.; Carlson, G. A. *Trends Biochem. Sci.* **2002**, *27*, 301−7.
[78]Drisaldi, B.; Coomaraswamy, J.; Mastrangelo, P.; Strome, B.; Yang, J.; Watts, J. C.; Chishti, M. A.; Marvi, M.; Windl, O.; Ahrens, R.; Major, F.; Sy, M. S.; Kretzschmar, H.; Fraser, P. E.; Mount, H. T.; Westaway, D. *J. Biol. Chem.* **2004**, *279*, 55443−54.